Properties of the pseudogap phase in high-T_c superconductors

A. A. Abrikosov
Materials Science Division, Argonne National Laboratory, 9700 South Cass Avenue, Argonne, Illinois 60439
(Received 11 April 2001; published 23 August 2001)

Several physical properties of the pseudogap phase are calculated on the basis of the spatially inhomogenous Franz-Millis model of superconducting fluctuations, consisting of small superconducting domains with uncorrelated supercurrents. The variation of this domain structure with time is supposed to be slow. A distribution function of superfluid velocities is found based on the assumption of the dominant role of extended saddle point singularities (''hot spots''). The model is used for calculation of the spectral function, the inelastic neutron scattering cross section, and the spin susceptibility entering the Knight shift. In all cases the calculated curves are qualitatively close to experimental results.

DOI: 10.1103/PhysRevB.64.104521 PACS number(s): 74.20.De, 74.20.Fg, 74.25.Dw, 74.62.Dh

I. INTRODUCTION

The last major unsolved problem in the theory of high-T_c superconducting cuprates (HTSC's) is the pseudogap, or more exactly, the pseudogap phase, which occurs in underdoped samples above T_c. It was first observed, as a ''spin gap'' in NMR experiments.[1] Then the new phase was found to influence various thermodynamic and kinetic phenomena, and finally, it clearly appeared in angle resolved photoemission spectroscopy (ARPES) experiments.[2,3] All these observations led to a conclusion that in underdoped samples in a certain temperature interval an unusual state appears, which has properties of both, the normal and superconducting, phases. Although we call it ''phase,'' as other authors do, it is not really a phase (such as, e.g., the ''vortex lattice''), since it is not separated from the normal state by a phase transition, and hence, does not differ from it by symmetry. It is possible, however, to speak about a crossover around some temperature T^*.

Most theorists agree that the pseudogap phase is due to fluctuations. There is, however, no agreement on their nature. Fluctuations can be of magnetic origin (spin fluctuations, see, e.g., Ref. 4), or of purely superconducting origin. The latter view was adopted in Refs. 5,6. In both approaches the superconductor was considered, as purely two-dimensional, and the hopping between the CuO_2 layers was not taken into account. This led to a problem in defining T_c, where a definite phase transition takes place.

One of the arguments, why the pseudogap is formed only in underdoped HTSC and not in conventional superconductors, or optimally doped and overdoped HTSC, was that the small electron concentration in underdoped samples makes them more vulnerable to fluctuations (see Ref. 6). This idea contradicts the fact that very thorough ARPES experiments[7] showed that the volume of the Fermi surface is large and changes very little with doping. Hence the concentration of holes is always large.

In our work[8] we proposed a solution of some of these mysteries. Here we will elaborate these ideas. First of all, we would like to describe in more detail some of our general assumptions. The large Fermi surface in the metallic state makes it extremely probable that the antiferromagnetic insulating phase is a spin-density wave existing in sufficiently pure samples at a proper electron concentration. I do not call it ''half-filling,'' since the Brillouin zone in the antiferromagnetic phase is one half of that in the metallic phase, and it is filled completely. Doping with oxygen decreases slightly the electron concentration and simultaneously creates disorder. Both changes are able to destroy the spin-density wave, and, as a result, a larger Brillouin zone appears, which is close to half filling. After that the volume of the Fermi surface does not change significantly with further doping. So the situation is radically different from doped semiconductors, where the crystalline lattice, and hence, the Brillouin zone does not change, and the dopant concentration defines the volume of the Fermi surface. Therefore, I find very misleading the rather commonly used name for the metallic phase: ''doped Mott insulator.''

If the concentration of carriers is large, and does not change significantly with further doping, what prevents this metal to become superconducting immediately after the transition, and to have a high critical temperature, as the optimaly doped samples? The idea, which was proposed in our papers[8,9] was based on the mechanism of interlayer connection due to resonant tunneling through oxygen atoms in the CuO chains, or BiO and TlO planes. These oxygen atoms are not only ''charge reservoirs'' but also resonant centers connecting the CuO_2 planes. The concentration of these atoms, contrary to the Fermi surface, is reduced drastically with underdoping, and the less the connection, the more two-dimensional becomes the material. Low dimensionality enhances fluctuations and destroys superconductivity. According to Refs. 8,9 this defines T_c in strongly underdoped samples and leads to its decrease with decreasing oxygen concentration.

In Ref. 8 we introduced the crossover temperature T^*, as the self-consistent BCS critical temperature. As we will see below, the real crossover happens at a temperature, which can be somewhat lower. In order to keep the usual notations, we call the BCS mean field critical temperature T^{**}. It could be found formally for any dimensionality but for low-dimensional systems it does not define a phase transition, since fluctuations destroy superconductivity. Our view is that T^{**} defines some ''hidden'' scale which has no explicit physical manifestations. As well known, in a *d*-wave superconductor ordinary, nonmagnetic, impurities strongly sup-

press the BCS critical temperature. In the process of doping disorder is introduced, and this leads to the decrease of T^{**}. In the overdoped region T^{**} approaches T_c (the phase diagram is presented in Fig. 1 of Ref. 8).

In this work we will consider the well developed pseudogap phase, i.e., the doping region, where the interval between T^{**} and T_c is large. If the temperature is not close to T_c, we can neglect hopping between the planes, and consider a purely two-dimensional model. We will use the model of Franz and Millis,[5] i.e., consider the metal, as an array of superconducting domains with different supercurrents. Leaving the more detailed description of the model to the next section we mention here only that we use a different distribution function for supercurrents reflecting the dominant role of extended saddle point singularities in the electron spectrum.

II. MODEL

As was said before, we will assume that the pseudogap phase is characterized by strong superconducting fluctuations. At every given moment the metal consists of small domains with different phases φ of the order parameter $\Psi = |\Psi| e^{i\varphi}$. Of course, this structure varies with time but we will assume that the characteristic measurement times are much shorter than the phase relaxation time. As far as the absolute value of the order parameter is concerned, we will suppose, the same, as in Refs. 5,6, that it does not vary over the whole sample, although it depends on temperature close to T^{**}.

According to experimental observations,[10,11] $\Delta_{\max}$ grows with T^* roughly following the BCS relation. We will assume that this relation holds for $\Delta_{\max}$ and T^{**}. If we neglect interplane hopping, the phase itself never enters the formulas. They contain only the gradient of the phase, which is proportional to the superfluid velocity (we use units with $\hbar=1$)

$$\mathbf{v}_s = \nabla\varphi/(2m). \tag{1}$$

Therefore, we can use the idea of Ref. 5 that the whole plane consists of domains with different superfluid currents. In every domain the variable $i\omega$ in the Green functions transforms to $i\omega - \mathbf{p}\mathbf{v}_s$ due to the Doppler effect, where $\mathbf{p}$ is the electron momentum (this was derived in Refs. 5,6 and could be obtained also from Ref. 12, sec. 19.2).

Here we must make a remark. The true expression is $i\omega - \frac{1}{2}\mathbf{v}\mathbf{q}$, where $\mathbf{v}$ is the Fermi velocity, and $\mathbf{q}$ is the momentum of Cooper pairs in a moving condensate. For an isotropic system both expressions are equivalent, provided that $\mathbf{p} = m\mathbf{v}$ and $\mathbf{q} = 2m\mathbf{v}_s$. However, for a real energy spectrum the electron quasimomentum is not a uniquely defined quantity, contrary to the Fermi velocity, and the latter is rather anisotropic in HTSC, becoming small in the vicinities of extended saddle point singularities in the electron energy spectrum (''hot spots''). As a result there is an increase of the density of states in these regions, and that makes them ''hot.'' For a simple quadratic spectrum in the singular region we get $v_1 = (2\mu_1/m)^{1/2}$, where $\mu_1 = \mu - \varepsilon_0$ is the chemical potential with respect to the bottom of the extended saddle point singularity.

As in the previous works (see Ref. 13, and references therein, we will assume that the singular regions, located close to $(\pi, 0)$, or $(-\pi,0)$ (we call them ''a''), and $(0,\pi)$, or $(0,-\pi)$ (we call them ''b''), are the most important. The distribution function of superfluid velocities we will assume as $W = e^{-F/T}$, where F is the free energy. The Ginzburg-Landau free energy for the model with extended saddle points was derived in Ref. 14. Leaving only terms depending on φ, we get

$$F = \frac{1}{4m}\int dxdy\left[|\Psi_a|^2\left(\frac{\partial\varphi_a}{\partial x}\right)^2 + |\Psi_b|^2\left(\frac{\partial\varphi_b}{\partial y}\right)^2\right]. \tag{2}$$

For a d-wave superconductor Ψ_a and Ψ_b differ only by their sign, and this difference vanishes here. Therefore we denote $|\Psi_a|^2 = |\Psi_b|^2 = \Psi_0^2$. The quantity Ψ_0^2, according to Ref. 14, is proportional to Δ_a^2, namely,

$$\Psi_0^2 \sim n[\Delta_a(T)/T^{**}]^2, \tag{3}$$

where n is the electron density in the singular region

$$n = \frac{m v_1 P_{y0}}{2\pi^2}. \tag{4}$$

Here P_{y0} is the length of the singularity in momentum space. Using relation (1), we substitute the phase gradients by components of $\mathbf{v}_s$. The integration in the plane, can be replaced by the characteristic area of the domain, where $\mathbf{v}_s$ remains constant. According to Ref. 15 (see, also, Ref. 8), the one-dimensional coherence length is $(\Delta_a^2 v_1/T^{**2}T)$. The characteristic area of a domain can be obtained, multiplying this by $2\pi/P_{y0}$.

After that we can write the distribution function

$$W[\mathbf{v}_s] = \exp\left[-\left(\frac{qm\mu_1\Delta_a^4(T)}{T^{**4}T^2}\right)\mathbf{v}_s^2\right], \tag{5}$$

where $q \sim 1$. This differs from the function derived in Ref. 5, which was based on the idea of Kosterlitz-Thouless spontaneous vortices. Strictly speaking, the v_{sx}^2 comes only from φ_a, and v_{sy}^2 only from φ_b but it is easy to understand that we can drop the indices ''a'' and ''b'' here. The coefficient at $m\mathbf{v}_s^2/T$ is generally of the order of unity, and it becomes small at $T \to T^{**}$. This is the reason, why the fluctuations are not small, and there is no real phase transition at T^{**}.

Until now we used the Ginzburg-Landau theory, which is valid in the vicinity of the critical temperature T^{**}. It is well known, however, that in the case of a short coherence length it coincides with the London theory, and the latter can be used at any temperature. The main assumption of the London theory is that in a superconductor the carriers (presently, Cooper pairs) behave, as free particles, and the free energy is essentially their kinetic energy. This corresponds exactly to what was assumed above.

The distribution (5) is true, if nothing limits $\mathbf{v}_s$. Actually, this is not the general case. There exists the Landau criterion

of superfluidity $v_s<\Delta/p$, which defines the critical current of very thin wires (see Ref. 12, Sec. 17.4). In principle, at larger velocities there could happen a phase transition to the normal state, or appear a resistive state with phase slip centers (see Ref. 12, Sec. 22.9). Here the Landau limit is

$$v_{sc}=\Delta_a(T)/(mv_1). \tag{6}$$

For now we use it only as a limitation, leaving a more detailed considerations of its consequences to Sec. V.

According to Eq. (5), the characteristic average value of v_s is

$$v_{sT}\sim\frac{T}{mv_1}\left(\frac{T^{**}}{\Delta_a(T)}\right)^2. \tag{7}$$

This should be compared with v_{sc}. If $v_{sT}\gg v_{sc}$, most of the volume is occupied by the normal phase. Therefore the condition $v_{sT}=v_{sc}$ defines the crossover temperature T^*. From Eqs. (6) and (7) we obtain $\Delta_a^3(T)\sim T^{**2}T$. The corresponding temperature is of the order of T^{**} but numerically it may be several times less. Therefore we assume that

$$T^*=rT^{**}, \tag{8}$$

with $r<1$.

III. ARPES SPECTRAL DENSITY

In the paper[16] it was shown that in the sum of the ARPES spectrum with its reflection with respect to the Fermi energy the Fermi function disappears, and the sum defines the spectral density of electrons for a given energy and momentum close to the Fermi level. We will use this conclusion, since it permits a direct comparison of the theory with experimental data. The spectral density is defined by the imaginary part of the retarded Green function

$$N(\omega,\mathbf{p})=-\frac{1}{\pi}\mathrm{Im}\,G^R(\omega,\mathbf{p}). \tag{9}$$

We will introduce more convenient variables for the momentum, namely, $\xi=v(p_\perp-p_0)$, and φ—the angle along the Fermi surface (we take a cylindrical Fermi surface with the Fermi momentum p_0, except for the small singular regions). The variable ω is the energy with respect to the chemical potential μ. The Doppler-shifted Green function was defined in Ref. 5:

$$G^R=\left(\omega-\eta-\xi+i\Gamma-\frac{\Delta^2(\varphi)}{\omega-\eta+\xi+i\Gamma}\right)^{-1}, \tag{10}$$

where $\eta=\mathbf{pv}_s$, and $\Delta(\varphi)$ is the absolute value of the self-consistent superconducting gap.

If we assume, as in Ref. 13, that $\Delta(\varphi)$ is defined by its values $\pm\Delta_a$ in the singular regions, then we obtain [here we take into account all four singular regions, *d*-wave symmetry, and for definiteness we assume $n=1$ in Eq. (5) of Ref. 13]

$$\frac{\Delta}{\Delta_a}=\frac{P_{y0}}{4dp_0^2\ln(P_{y0}/\kappa)}\left([\sin^2(\varphi/2)+\mathbf{a}]^{-1}\right.$$
$$+\{\sin^2[(\pi-\varphi)/2]+\mathbf{a}\}^{-1}-\{\sin^2[(\pi/2-\varphi)/2]+\mathbf{a}\}^{-1}$$
$$\left.-\{\sin^2[(3\pi/2-\varphi)/2]+\mathbf{a}\}^{-1}\right). \tag{11}$$

Here d is the interlayer spacing, κ is the reciprocal Debye screening radius, P_{y0} is the length of the singular region, and $\mathbf{a}$ is an interpolation constant, chosen so that at $\varphi=0$ $\Delta=\Delta_a$. It is supposed that $\Delta(\varphi)$ is large only in the singular regions, and therefore the small constant $\mathbf{a}$ is approximately equal to the prefactor in formula (11). Simplifying the expression (11) we get

$$\frac{\Delta(\varphi)}{\Delta_1}=\frac{\cos 2\varphi}{1+Q\sin^2 2\varphi};\quad Q\approx\frac{1}{16\mathbf{a}}\approx\frac{dp_0^2\ln(P_{y0}/\kappa)}{4P_{y0}}\gg 1. \tag{12}$$

If the damping Γ is small, the imaginary part of G^R is a δ function

$$-\frac{1}{\pi}\mathrm{Im}\,G^R=\delta\left(\omega-\eta-\xi-\frac{\Delta^2(\varphi)}{\omega-\eta+\xi}\right)$$
$$=v_B^2\delta(\eta-\omega-\varepsilon)+u_B^2\delta(\eta-\omega+\varepsilon), \tag{13}$$

where u_B, v_B are the Bogoliubov transformation coefficients

$$u_B^2, v_B^2=\frac{1}{2}\left(1\pm\frac{\xi}{\varepsilon}\right)$$

and

$$\varepsilon=[\xi^2+\Delta^2(\varphi)]^{1/2}.$$

We will be mostly interested in the vicinities of ''nodes,'' i.e., regions far from the singularities. Therefore

$$\eta=p_xv_{sx}+p_yv_{sy}=p_0(v_{sx}\cos\varphi+v_{sy}\sin\varphi), \tag{14}$$

where $p_0=mv_0$ is the large Fermi momentum.

Expression (13) has to be averaged over the distribution of velocities (5). We will assume that the temperature is sufficiently below T^*, and the Landau criterion plays no role. Then the limits for the v_{sx} and v_{sy} integrations can be taken, as infinite. Instead of v_{sx}, v_{sy} we will introduce variables η and ζ, where η is defined by Eq. (14), and $\zeta=p_0(-v_{sx}\sin\varphi+v_{sy}\cos\varphi)$. Since this is a change of scale and a rotation, we get $v_{sx}^2+v_{sy}^2=(\eta^2+\zeta^2)/p_0^2$ and $dv_{sx}dv_{sy}\to d\eta d\zeta/p_0^2$. Integrating over η and ζ and dividing by $\int W[\mathbf{v}_s]dv_{sx}dv_{sy}$, we get

$$-\frac{1}{\pi}\langle\mathrm{Im}\,G^R\rangle=\left(\frac{A}{\pi}\right)^{1/2}\{v_B^2[\xi,\Delta(\varphi)]\exp[-A(\omega+\varepsilon)^2]$$
$$+u_B^2[\xi,\Delta(\varphi)]\exp[-A(\omega-\varepsilon)^2]\}, \tag{15}$$

where

$$A=q\frac{\mu_1\Delta^4}{\mu T^{**4}T^2},\quad \mu=p_0^2 2m,\quad \Delta\equiv\Delta_a(T=0). \tag{16}$$

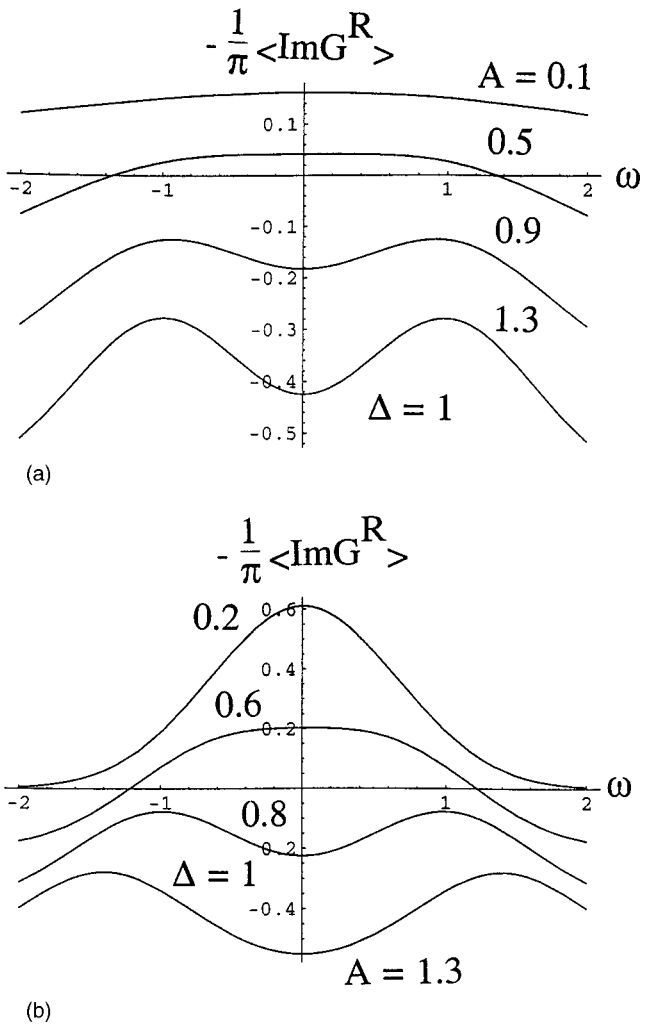

FIG. 1. Spectral density at the Fermi surface, as function of energy: (a) fixed Δ (i.e., angle φ) and different values of A (i.e., temperatures); (b) fixed A and different Δ.

Formula (15) is general, and describes the dependence of the spectral function on energy ω and momentum (ξ and φ). In order to make the result more transparent we will consider a particular case, namely, the momentum exactly at the Fermi surface, or $\xi=0$. In this case formula (15) simplifies:

$$-\frac{1}{\pi}\langle \mathrm{Im}\, G^R\rangle = \frac{1}{2}\left(\frac{A}{\pi}\right)^{1/2}(\exp\{-A[\omega+\Delta(\varphi)]^2\} + \exp\{-A[\omega-\Delta(\varphi)]^2\}). \tag{17}$$

The example of the spectral density is presented in Fig. 1. Here Fig. 1(a) are the curves for a fixed $\Delta=1$ and different values of A (0.1–1.3), i.e., for different temperatures, and Fig. 1(b) are the curves for a fixed $A=1.3$ but different $\Delta(\varphi)$ (0.2–1), i.e., for different angles φ. In the general case we have a two-peaked curve resembling the experimental results of Ref. 15.

There are many ways to define the pseudogap. The most natural way is to define it, as a half-distance between the maxima of the curve (17). The pseudogap disappears, when the two maxima merge together, and the corresponding condition is that the second derivative with respect to ω vanishes at $\omega=0$. This happens at

$$|\Delta(\varphi)| = (2A)^{-1/2} = \left(\frac{\mu}{2q\mu_1}\right)^{1/2}\left(\frac{\Delta}{T^{**}}\right)^2 T. \tag{18}$$

We see that with increasing temperature the pseudogap disappears in an increasing angular range around the nodes. This qualitatively fits the experimental data of Ref. 16. Of course, our derivation fails close to T^* and close to the real superconducting transition, where hopping between planes becomes important.

IV. THE NEUTRON MAXIMUM

One of the most spectacular phenomena in the physics of HTSC's is the maximum in the inelastic neutron scattering cross section, as function of the loss of energy and momentum by the neutron. The maximum is sharp in the superconducting phase. However, a smooth maximum exists also in the pseudogap phase.[17] In Refs. 18,19 we have calculated the imaginary part of the electron spin susceptibility, as function of momentum and energy, which can be extracted from the inelastic spin-flip neutron scattering cross section. The calculations were done for the superconducting phase in the model with the dominant role of extended saddle point singularities. Fluctuations were not taken into account, and so, the corresponding object was an optimally doped, or overdoped, superconductor below T_c (for simplicity we assumed $T=0$).

Here we will do the calculation for the pseudogap phase at temperatures lower than T^*; therefore the Landau criterion will be neglected. We will analyze only the energy dependence and use the simplest model of Ref. 18. Since in the scattering process the electron hops from the vicinity of one singularity to the other one, these vicinities are the most important regions also in the present calculation. Therefore in formula (16) for A μ has to be replaced by μ_1. After that we have $A\to A_1$, where

$$A_1 = q_1\left(\frac{\Delta_a^2(T)}{T^{**2}T}\right)^2, \tag{19}$$

and q_1 is another constant of the order of unity. Since we presumed that the temperature is lower than T^*, $\Delta_a(T)\sim\Delta \sim T^{**}$, and $A_1\Delta^2\sim(T^{**}/T)^2\geqq 1$. We start with formula (1) in Ref. 18. According to the preceding sections, we have to replace in all "a" Green functions $i\omega$ by $i\omega-\eta_x$, and in the "b" functions $i(\omega-\Omega)$ by $i(\omega-\Omega)-\eta_y$, where $\eta_x,\eta_y = mv_1(v_{sx},v_{sy})$. This has to be averaged over η_x and η_y with the weight

$$(A_1/\pi)\exp[-A_1(\eta_x^2+\eta_y^2)]. \tag{20}$$

Summation over frequencies leads to a formula resembling Eq. (2) in Ref. 18:

$$\chi=\int (A_1/\pi)\exp[-A_1(\eta_x^2+\eta_y^2)]d\eta_x d\eta_y \int dp_x dp_y (2\pi)^{-2} d^{-1}$$

$$\times\left\{\frac{1}{4\varepsilon_a}\left[\tanh\frac{\varepsilon_a+\eta_x}{2T}\,\frac{(\varepsilon_a+\xi_a)(\varepsilon_a+\eta_x-\Omega-\eta_y+\xi_b)-\Delta^2}{(\varepsilon_a+\eta_x-\Omega-i\delta-\eta_y)^2-\varepsilon_b^2}+\tanh\frac{\varepsilon_a-\eta_x}{2T}\,\frac{(\varepsilon_a-\xi_a)(\varepsilon_a-\eta_x+\Omega+\eta_y-\xi_b)-\Delta^2}{(\varepsilon_a-\eta_x+\Omega+i\delta+\eta_y)^2-\varepsilon_b^2}\right]\right.$$

$$\left.+\frac{1}{4\varepsilon_b}\left[\tanh\frac{\varepsilon_b+\eta_y}{2T}\,\frac{(\varepsilon_b+\xi_b)(\varepsilon_b-\eta_x+\Omega+\eta_y+\xi_a)-\Delta^2}{(\varepsilon_b-\eta_x+\Omega+i\delta+\eta_y)^2-\varepsilon_a^2}+\tanh\frac{\varepsilon_b-\eta_y}{2T}\,\frac{(\varepsilon_b-\xi_b)(\varepsilon_b+\eta_x-\Omega-\eta_y-\xi_a)-\Delta^2}{(\varepsilon_b+\eta_x-\Omega-i\delta-\eta_y)^2-\varepsilon_a^2}\right]\right\}. \tag{21}$$

Substituting $\xi_b \rightleftarrows -\xi_a$, $\eta_y \rightleftarrows -\eta_x$ in the second term, we obtain

$$\chi=\int (A_1/\pi)\exp[-A_1(\eta_x^2+\eta_y^2)]d\eta_x d\eta_y \int dp_x dp_y (2\pi)^{-2} d^{-1}$$

$$\times\left\{\frac{1}{2\varepsilon_a}\left[\tanh\frac{\varepsilon_a+\eta_x}{2T}\,\frac{(\varepsilon_a+\xi_a)(\varepsilon_a+\eta_x-\Omega-\eta_y+\xi_b)-\Delta^2}{(\varepsilon_a+\eta_x-\Omega-i\delta-\eta_y)^2-\varepsilon_b^2}+\tanh\frac{\varepsilon_a-\eta_x}{2T}\,\frac{(\varepsilon_a-\xi_a)(\varepsilon_a-\eta_x+\Omega+\eta_y-\xi_b)-\Delta^2}{(\varepsilon_a-\eta_x+\Omega+i\delta+\eta_y)^2-\varepsilon_b^2}\right]\right\}. \tag{22}$$

Performing the integration over p_y we act in the same way, as in Ref. 18. Since we are interested in χ'', we leave only the integration over half-circles around the poles. For simplicity we consider only the case of $\mu_1=0$. Hence, we may neglect the integration over negative ξ_b and omit μ_1 in the denominators. After that we pass from integration over p_x to the integration over ξ_a leaving again only the positive part. Everywhere we replace $\tanh(x/2T)$ by $\mathrm{sgn}(x)$. The result is

$$\chi''=\int (A_1/\pi)\exp[-A_1(\eta_x^2+\eta_y^2)]d\eta_x d\eta_y$$

$$\times\frac{m}{4\pi d}\left\{\int d\varepsilon\ \mathrm{sgn}(\varepsilon-\Omega+\eta)\mathrm{sgn}(\varepsilon+\eta_x)\right.$$

$$\times\frac{[\varepsilon+|\xi(\varepsilon)|][\varepsilon-\Omega+\eta+|\xi(\varepsilon-\Omega+\eta)|]-\Delta^2}{|\xi(\varepsilon)|^{3/2}|\xi(\varepsilon-\Omega+\eta)|^{3/2}}$$

$$-\int d\varepsilon\ \mathrm{sgn}(\varepsilon+\Omega-\eta)\mathrm{sgn}(\varepsilon-\eta_x)$$

$$\left.\times\frac{[\varepsilon-|\xi(\varepsilon)|][\varepsilon+\Omega-\eta-|\xi(\varepsilon+\Omega-\eta)|]-\Delta^2}{|\xi(\varepsilon)|^{3/2}|\xi(\varepsilon+\Omega-\eta)|^{3/2}}\right\}, \tag{23}$$

where $\eta=\eta_x-\eta_y$, $|\xi(\varepsilon)|=(\varepsilon^2-\Delta^2)^{1/2}$.

Since there is a separate dependence on η_x, we will introduce new variables η and $\zeta=\eta_x+\eta_y$. It is easy to see that $\eta_x^2+\eta_y^2=(1/2)(\eta^2+\zeta^2)$, and $d\eta_x d\eta_y=(1/2)d\eta d\zeta$. Substituting $\eta_x=(\eta+\zeta)/2$, we can integrate over $d\zeta$. After that we have

$$\int \mathrm{sgn}[\varepsilon+(\eta+\zeta)/2]\exp(-A_1\zeta^2/2)d\zeta$$

$$=(2\pi/A_1)^{1/2}\Phi[(A_1/2)^{1/2}(2\varepsilon+\eta)], \tag{24}$$

where Φ is the error function.

The integration limits over ε in Eq. (23) are defined so that the ξ are real, i.e., their arguments have an absolute value larger than Δ. The maximum appears, if one of the arguments is larger than Δ, and the other is smaller than $-\Delta$ (as in Refs. 18 and 19; we call this part χ''_m). Since $\varepsilon>\Delta$, we must have $\varepsilon-\Omega+\eta<-\Delta$ in the first term of Eq. (23), and $\varepsilon+\Omega-\eta<-\Delta$ in the second. Hence the limits for the first term are $\Delta<\varepsilon<\Omega-\eta-\Delta$, and for the second one they are $\Delta<\varepsilon<\eta-\Omega-\Delta$. From here we can decide that the integration over η in the first term is within limits $-\infty<\eta<\Omega-2\Delta$, and for the second it is within $\Omega+2\Delta<\eta<\infty$. We will introduce instead of ε a new variable $\rho=\varepsilon+(\Omega-\eta)/2$ in the first term of Eq. (23) and $\rho_1=\varepsilon+(\eta-\Omega)/2$ in the second term. The corresponding integrands are even functions of ρ and ρ_1 and the integration limits are symmetrical. This permits to pass to the integration over positive values of the corresponding variable. Eventually we get

$$\chi_m''=\frac{m}{4\pi d}\left(\frac{A_1}{2\pi}\right)^{1/2}\int_{-\infty}^{\Omega-2\Delta}\exp[-A_1\eta^2/2]d\eta\int_0^{z-\Delta}d\rho\,\frac{z^2-\rho^2+\Delta^2-[(z^2-\rho^2)^2-2\Delta^2(z^2+\rho^2)+\Delta^4]^{1/2}}{[(z^2-\rho^2)^2-2\Delta^2(z^2+\rho^2)+\Delta^4]^{3/4}}$$
$$\times\{\Phi[(A_1/2)^{1/2}(\Omega+2\rho)]+\Phi[(A_1/2)^{1/2}(\Omega-2\rho)]\}-\frac{m}{4\pi d}\left(\frac{A_1}{2\pi}\right)^{1/2}$$
$$\times\int_{\Omega+2\Delta}^{\infty}\exp[-A_1\eta^2/2]d\eta\int_0^{z_1-\Delta}d\rho\,\frac{z_1^2-\rho^2+\Delta^2-[(z_1^2-\rho^2)^2-2\Delta^2(z_1^2+\rho^2)+\Delta^4]^{1/2}}{[(z_1^2-\rho^2)^2-2\Delta^2(z_1^2+\rho^2)+\Delta^4]^{3/4}}$$
$$\times\{\Phi[(A_1/2)^{1/2}(\Omega+2\rho)]+\Phi[(A_1/2)^{1/2}(\Omega-2\rho)]\},\qquad(25)$$

where $z=-z_1=(\Omega-\eta)/2$. It is easy to see that the second term transforms into the first one, if we substitute Ω by $-\Omega$ and change the integration variable η to $-\eta$. Hence, $\chi_m''=F(\Omega)+F(-\Omega)$, where $F(\Omega)$ is the first term in Eq. (25).

As it was said before, the real physical situation corresponds to $A_1\Delta^2\geqslant 1$. Let us first suppose $A_1\Delta^2\gg 1$. Then the result will be a slight smear-out of formulas (7),(8) from Ref. 18. The maximum will appear at $\Omega\approx 2\Delta$, and since the important η will also be small, the upper limit of the ρ integration in the first integral of Eq. (25) will be small. This leads to simplifications, and after performing the integration over ρ in the first term of Eq. (25) we get

$$F(\Omega)=\frac{ma}{2\pi d}\left(\frac{A_1}{2\pi}\right)^{1/2}\int_{-\infty}^{\Omega-2\Delta}\times\exp\left(-\frac{A_1\eta^2}{2}\right)\sqrt{\frac{2\Delta}{\Omega-2\Delta-\eta}}d\eta,\qquad(26)$$

where

$$a=\frac{[\Gamma(1/4)]^2}{4\sqrt{\pi}}=1.8541.$$

Introducing new variables $\omega=(A_1/2)^{1/2}\Omega$, $\delta=(A_1/2)^{1/2}\Delta$ and passing to the integration over $u=(A_1/2)^{1/4}(\Omega-2\Delta-\eta)^{1/2}$ we obtain for $F(\Omega)$

$$F(\Omega)=\chi_m''=\frac{m\Gamma^2(1/4)}{2^{3/2}\pi^2 d}\,\delta^{1/2}P(\omega-2\delta),$$
$$P(x)=\int_0^{\infty}\exp[-(x-u^2)^2]du.\qquad(27)$$

We wrote $F(\Omega)=\chi_m''$, since the second term of Eq. (25) has the relative order of magnitude $\exp[-A_1(\Omega+2\Delta)^2/2]\ll 1$. The asymptotic formulas for the function $P(x)$ are

$$P(x)\approx\begin{cases}\left(\dfrac{\pi}{4x}\right)^{1/2}, & x\gg 1,\\ 0.9064+0.6027x-0.5468x^2, & |x|\ll 1,\\ \left(\dfrac{\pi}{8|x|}\right)^{1/2}\exp(-|x|^2), & x<0,\ |x|\gg 1.\end{cases}\qquad(28)$$

The full plot of $P(x)$ is presented in Fig. 2.

In order to have a better idea about the behavior of χ_m'' at intermediate values of $A_1\Delta^2$ we calculate it for $A_1\Delta^2\ll 1$, although this case has no real physical relevance. For this case in Eq. (25) we can neglect Δ compared to z, although not compared to $\rho-z$. Performing the integration with respect to ρ in the first term of Eq. (25) we obtain

$$F(\Omega)=\frac{mb}{4\pi d}\left(\frac{A_1}{2\pi}\right)^{1/2}\int_{-\infty}^{\Omega-2\Delta}d\eta\exp[-A_1\eta^2/2]\sqrt{\frac{2\Delta}{\Omega-\eta}}$$
$$\times\{\Phi[(A_1/2)^{1/2}(2\Omega-\eta)]+\Phi[(A_1/2)^{1/2}\eta]\},\qquad(29)$$

where

$$b=2\int_0^1\frac{x^2dx}{(1-x^4)^{1/2}}=2\sqrt{2}\left[E(1/\sqrt{2})-\frac{1}{2}F(1/\sqrt{2})\right]=1.198.$$

Here $E(k)$ and $F(k)$ are complete elliptic integrals [in "MATHEMATICA" the notation "Elliptic$E[m]$" means $E(\sqrt{m})$]. We introduce the variable $\omega=(A_1/2)^{1/2}\Omega$, take the symmetric combination $F(\Omega)+F(-\Omega)$ and use the integration variable $u=(A_1/2)^{1/4}(\Omega-\eta)^{1/2}$. After that we get

$$\chi_m''=\frac{bm(2A_1)^{1/4}\Delta^{1/2}}{2\pi^{3/2}d}Q(\omega),$$

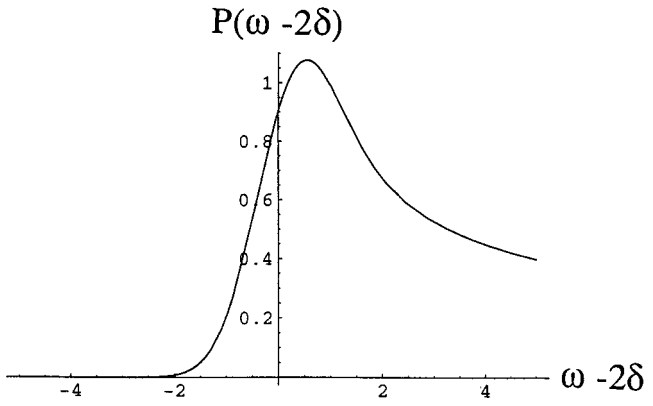

FIG. 2. Shape of the maximum in the inelastic neutron scattering cross section above T_c in the case of small fluctuations ($A_1\Delta^2\gg 1$): function $P(\omega-2\delta)$ [formula (27)].

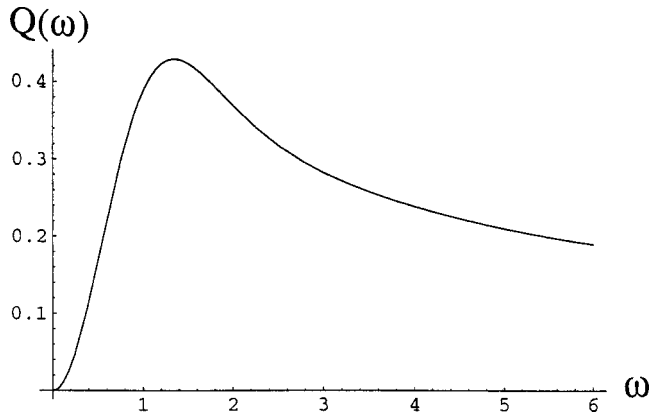

FIG. 3. Shape of the maximum in the inelastic neutron scattering cross section above T_c in the case of large fluctuations ($A_1\Delta^2 \ll 1$): function $Q(\omega)$ [formula (30)].

$$Q(\omega)=\int_0^\infty du\,\exp(-\omega^2-u^4)\sinh(2\omega u^2) \times\Phi(u^2-\omega,u^2+\omega), \tag{30}$$

where $\Phi(x_1,x_2)=\Phi(x_2)-\Phi(x_1)$. The asymptotic forms of the integral $Q(\omega)$ are

$$Q(\omega)=\begin{cases}\dfrac{8\omega^2}{\sqrt{\pi}}\displaystyle\int_0^\infty x^2\exp(-2x^4)dx=0.822\omega^2, & \omega\ll 1\\ \dfrac{1}{4}\sqrt{\dfrac{\pi}{\omega}}=\dfrac{0.443}{\sqrt{\omega}}, & \omega\gg 1.\end{cases} \tag{31}$$

The full curve for $Q(\omega)$ is presented in Fig. 3. The curves in Figs. 2 and 3 resemble each other. From this one can conclude that for the intermediate case $A_1\Delta^2\sim 1$ the curve will have essentially the same features. On the other hand, these curves resemble the experimental data for the normal region of underdoped samples (see Ref. 17, Fig. 9). There the data for different dopings were taken at the same temperature. Since the T^{**} grows with underdoping, the same should be true for the location of the maximum, and such a trend, indeed, exists.

V. THE SPIN GAP

As was said in the introduction, the ''spin gap'' appears in the NMR experiments, as a gaplike feature in the temperature dependence of the Knight shift and the spin relaxation rate.[1] Particularly, the Knight shift starts to decrease with decreasing temperature high above T_c. We will calculate here the spin susceptibility, which defines the temperature dependence of the Knight shift. The central idea of this calculation is that the appearance of the normal regions is due mostly to the violation of the Landau criterion.

This requires some explanation. As we mentioned previously, due to the ''extended saddle point singularities,'' the most important electrons are, actually, one dimensional. In the Appendix a calculation is presented for the ''self-consistent'' critical velocity in one dimension. From that calculation one can see that there are two possibilities. The transition can be of the second order, and then the order parameter gradually (but rather steeply) decreases with increasing superfluid velocity, until it vanishes. Another option is that the current reaches a maximum at a finite value of the order parameter. In a thin wire this would mean the appearance of a resistive state with phase slip centers, where the order parameter vanishes periodically with time, and the supercurrent is then replaced by a normal current. Of course, in fluctuations which we consider here the situation could be different, since they happen in a plane, but these two options give us an idea of a rough but simple model which can describe the consequences of the Landau criterion. We assume that the order parameter does not depend on the superfluid velocity up to the Landau limit, and after that it vanishes discontinuously. The velocity distribution continues beyond the Landau limit (this simulates the resistive state). This model gives a rather realistic description of the Knight shift, as can be seen below.

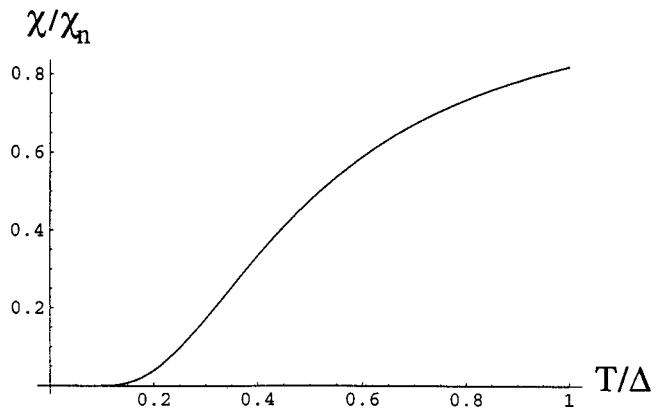

FIG. 4. The relative spin susceptibility χ/χ_n as function of T/Δ in the case of small fluctuations $\alpha\gg 1$ [formula (35)].

Since the spin susceptibility is proportional to the density of states, and the latter is maximal in the singular regions we will consider only them, as it was done in Refs. 20 and 21. The contributions of the regions ''*a*'' and ''*b*'' are equal for a tetragonal metal, and so we consider only one of them and double the result. The susceptibility, divided by μ_B^2 (square of the Bohr magneton), is

$$\chi[\eta]=-2T\sum_\omega\int\frac{d^2\mathbf{p}}{(2\pi)^2 d}\,\frac{(i\omega-\eta+\xi)^2+\Delta^2}{[(i\omega-\eta)^2-\varepsilon^2]^2}. \tag{32}$$

Performing summation over ω, and passing to the variable ξ, we obtain

$$\chi[\eta]=\frac{P_{y0}}{\pi^2 v_1 d}\int_0^\infty\frac{d\xi}{2T}\{\cosh^{-2}[(\varepsilon-\eta)/2T] +\cosh^{-2}[(\varepsilon+\eta)/2T]\}, \tag{33}$$

where P_{y0} is the width of the singular region. Dividing this by the value in the normal state (with $\varepsilon\to\xi$) and averaging over η with the weight $(A_1/\pi)^{1/2}\exp(-A_1\eta)^2$ (see Sec. IV) we get

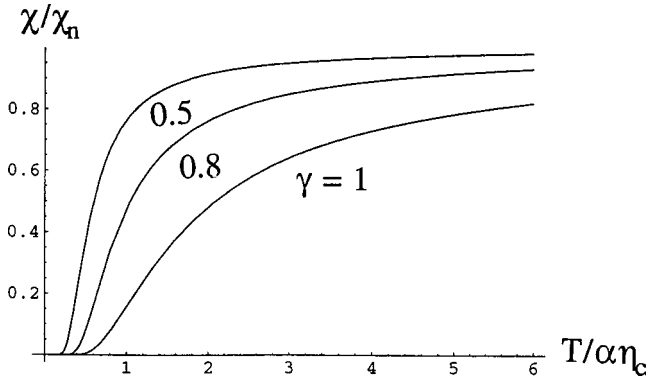

FIG. 5. The relative spin susceptibility χ/χ_n as function of $T/(\alpha\eta_c)$ for different values of $\gamma=\Delta/(\alpha\eta_c)$ in the case of large fluctuations, $\alpha\ll 1$ [formula (37)].

$$\chi/\chi_n = 2(A_1/\pi)^{1/2}\int_0^\infty d\eta \exp(-A_1\eta^2) \times \int_0^\infty \frac{d\xi}{4T}\{\cosh^{-2}[(\varepsilon-\eta)/2T] + \cosh^{-2}[(\varepsilon+\eta)/2T]\}. \quad (34)$$

According to our model, a substitution $\varepsilon\to\xi$ should be done in the integral over $\eta>\eta_c\sim\Delta_a(T)$ [see Eq. (6)]

The integral (34) contains two δ-like functions. The width of one of them is T, and of the other one is $A_1^{-1/2}$. According to the definition (19),

$$\alpha = TA_1^{1/2}\sim[\Delta_a(T)/T^{**}]^2 \quad (35)$$

this ratio is never large and close to T^{**} it can be small. We will consider temperatures $T<T^{**}$, and therefore $\Delta_a(T)\sim\Delta$. Hence both, the ratio (35), as well as η_c/Δ, are formally of the order of unity. Using the definition (35) and switching to new variables, we will write formula (34) in the form

$$\chi/\chi_n = \frac{2}{\sqrt{\pi}}\left\{\int_0^{\alpha\eta_c/T} du\exp(-u^2) \times \int_0^\infty \frac{dx}{4}\cosh^{-2}[(\zeta-u/\alpha)/2]+\cosh^{-2}[(\zeta+u/\alpha)/2] + \int_{\alpha\eta_c/T}^\infty du\exp(-u^2)\right\}, \quad (36)$$

where $x=\xi/T$, $\zeta=[x^2+(\Delta/T)^2]^{1/2}$ (we have performed the x-integration in the second term, using $\Delta=0$). This is the general formula depending on three adjustable parameters: α, the temperature scale, e.g., $\alpha\eta_c$ and the ratio Δ/η_c.

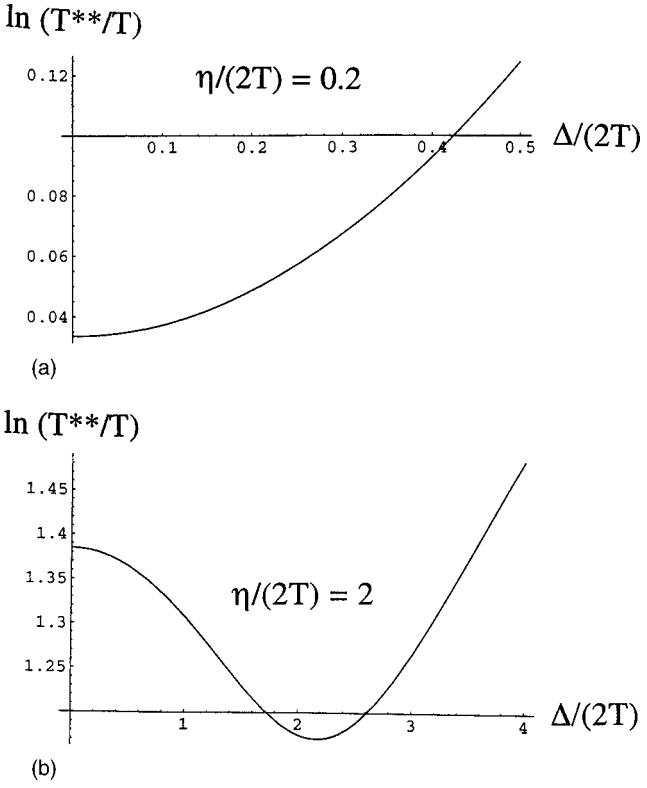

FIG. 6. Calculation of the critical current. Plot of $\ln(T^{**}/T)$ as function of $x=\Delta/(2T)$: (a) at $y=\eta/(2T)=0.2$; the minimum corresponds to $x=0$, (b) at $y=2$; the minimum corresponds $x\neq 0$.

In order to have an idea of the shape of this dependence, we consider the limiting cases: $\alpha\gg 1$, and $\alpha\ll 1$. In the first case we can neglect the second term in Eq. (36), and in the first term we put everywhere $\alpha=\infty$. This, actually, means that fluctuations are negligible, and the Landau mechanism does not work. We get the usual superconducting formula for the region, where Δ does not depend on temperature. The corresponding plot of $\chi/\chi_n(T/\Delta)$ is presented in Fig. 4.

In the opposite case $\alpha\ll 1$ we can substitute $(1/4)\cosh^{-2}[(\zeta-u/\alpha)/2]$ by $\delta(\zeta-u/\alpha)$ and neglect $\cosh^{-2}[(\zeta+u/\alpha)/2]$. After that the result becomes $\chi/\chi_n = R(T/\alpha\eta_c)$,

$$R(x) = 1+\theta(1-\gamma)\exp[-(\gamma/x)^2]\Phi[(1-\gamma^2)^{1/2}/x] - \Phi(1/x), \quad (37)$$

where $\gamma=\Delta/\eta_c$ and Φ is the error function. The asymptotic formulas for $R(x)$ are

$$R(x)\approx\begin{cases}\theta(1-\gamma)\exp(-\gamma^2/x^2)-(x/\sqrt{\pi})\exp(-1/x^2)[\theta(1-\gamma)/(1-\gamma^2)^{1/2}-1], & x\ll 1,\\ 1-(2/\sqrt{\pi x})[1-\theta(1-\gamma)(1-\gamma^2)^{1/2}], & x\gg 1.\end{cases} \quad (38)$$

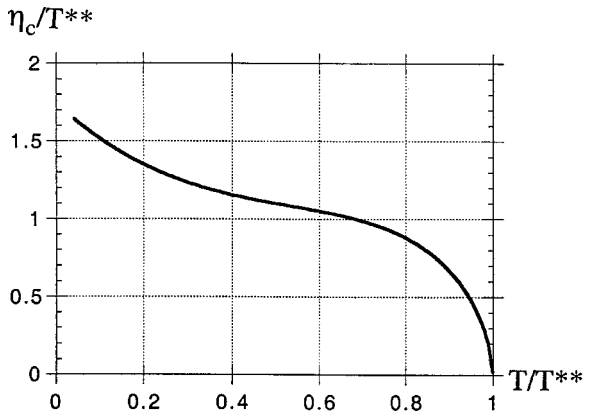

FIG. 7. The critical value of η_c/T^{**}, as function of reduced temperature T/T^{**}.

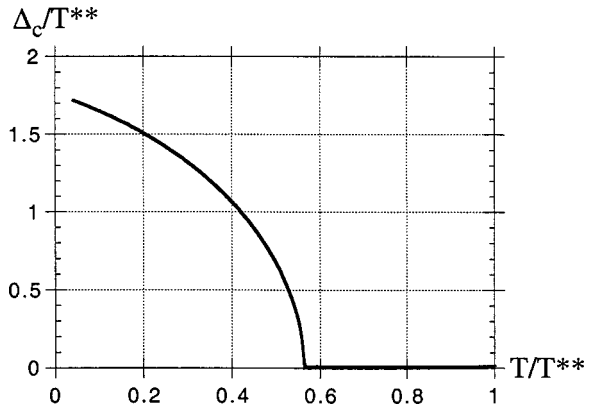

FIG. 8. The value of Δ_c/T^{**} at the critical value of the current, as function of reduced temperature. At higher temperatures it is zero, i.e., there is a second order phase transition, and at temperatures below the tricritical point the finite value manifests a first order transition.

The complete plot of the function $R(x)$ for several values of γ is presented in Fig. 5. Comparison with the experimental results[1] shows close resemblance.

VI. CONCLUSIONS

As was mentioned in Secs. III–V the results of theoretical calculations based on the Franz-Millis model with the Gaussian distribution function for one-dimensional fluctuations fit qualitatively well the experimental observations. The number of adjustable parameters is sufficient for a quantitative fit but this was not our goal. The model has some limitations. The main of them is that we have not considered interplane hopping, and this makes it inapplicable to temperatures close to T_c.

Fluctuations exist also in the superconducting phase, and taking them into account is important. One of the examples is that the energy of the neutron maximum in the superconducting state with underdoping varies proportional to the real T_c, i.e., decreases, whereas the gap, measured by the maximum in the ARPES spectrum increases. Both maxima are rather sharp. The deficiency of the model can be clearly understood from the fact that the hopping between planes leads to a Josephson energy depending on the phases of the order parameter at different planes, and not only on their gradients. Therefore, the description in terms of supercurrents is no more valid, if we approach T_c. The construction of the theory in this vicinity will be the subject of future work.

ACKNOWLEDGMENT

This work was supported by the U.S. Department of Energy under Contract No. W-31-109-ENG-38.

APPENDIX: SELF-CONSISTENT CRITICAL CURRENT IN ONE DIMENSION

In order to understand better the Landau criterion, we will find here the critical current in the mean field approximation, when the current is directed along one of the axes (1,0) or (0,1). In this case we can consider the problem, as one dimensional. Introducing a moving Bose condensate, as before, we use a derivation similar to Ref. 12, Sec. 16.5. In this way we obtain

$$\ln\frac{T^{**}}{T}=\int_0^\infty d\xi\left(\frac{1}{\xi}\tanh\frac{\xi}{2T}-\frac{1}{2\varepsilon}\tanh\frac{\varepsilon+\eta}{2T}-\frac{1}{2\varepsilon}\tanh\frac{\varepsilon-\eta}{2T}\right), \tag{A1}$$

where $\varepsilon=(\xi^2+\Delta^2)^{1/2}$. From this formula it is possible to define the maximal value of η at any temperature and the corresponding value of Δ. For this purpose we fix a certain value of $y=\eta/2T$ and calculate the right hand side of Eq. (A1), as function of $x=\Delta/2T$. It will be either a monotonous function of x with a minimum at $x=0$, or have a minimum at some finite value of x. Examples are given in Fig. 6: (a) $y=0.2$, (b) $y=2$. From the coordinates of the minimum we define $\Delta_c/2T$ and $\ln(T^{**}/T)$, and from that the corresponding η_c/T^{**} and Δ_c/T^{**}. Figures 7 and 8 show both quantities, as functions of T/T^{**}. One can clearly see that the phase transition at $T/T^{**}>0.5645$ is a second order transition, and at lower temperatures it becomes a first order transition.

Another problem is connected with magnetic fluctuations. Recent observations[22,23] permitted us to establish the existence of antiferromagnetic ordering in underdoped YBCO above the Neél temperature, both, in the superconducting and in the pseudogap phase. Since the magnetic moments are small, and the magnetization fluctuates with time, this phenomenon, has, probably, no influence on many properties, including those, calculated above, but it has to be explained. I think that it may provide a confirmation of the idea on the nature of the metal-insulator transition described in the Introduction.

[1] M. Takigawa, A. P. Reyes, P. C. Hammel, J. D. Thompson, R. H. Heffner, Z. Fisk, and K. C. Ott, Phys. Rev. B **43**, 247 (1991).
[2] H. Ding, T. Yokoya, J.-C. Campuzano, T. Takahashi, M. Randeria, M. R. Norman, T. Mochiku, K. Kadowaki, and J. Giapintzakis, Nature (London) **382**, 51 (1996).
[3] A. G. Loeser, Z. X. Shen, D. S. Dessau, D. S. Marshall, C. H. Park, P. Fournier, and A. Kapitulnik, Science **273**, 325 (1996).
[4] A. V. Chubukov and J. Schmalian, Phys. Rev. B **57**, R11 085 (1998).
[5] M. Franz and A. J. Millis, Phys. Rev. B **58**, 14 572 (1998).
[6] H.-J. Kwon and A. T. Dorsey, Phys. Rev. B **59**, 6438 (1999).
[7] H. Ding, M. R. Norman, T. Yokoya, T. Takeuchi, M. Randeria, J.-C. Campuzano, T. Takahashi, T. Mochiku, and K. Kadowaki, Phys. Rev. Lett. **78**, 2628 (1997).
[8] A. A. Abrikosov, Phys. Rev. B **63**, 134518 (2001).
[9] A. A. Abrikosov, Physica C **317–318**, 154 (1999).
[10] N. Miyakawa, P. Guptasarma, J. F. Zasadzinski, D. G. Hinks, and K. E. Gray, Phys. Rev. Lett. **80**, 157 (1998).
[11] H. Ding, J.-C. Campuzano, M. R. Norman, M. Randeria, T. Yokoya, T. Takahashi, T. Takeuchi, T. Mochiku, K. Kadowaki, P. Guptasarma, and D. Hinks, J. Phys. Chem. Solids **59**, 1888 (1998).
[12] A. A. Abrikosov, *Fundamentals of the Theory of Metals* (North-Holland, Amsterdam, 1988).
[13] A. A. Abrikosov, Physica C **341–348**, 97 (2000).
[14] A. A. Abrikosov, Phys. Rev. B **56**, 446 (1997).
[15] T. M. Rice, Phys. Rev. A **140**, 1889 (1965).
[16] M. R. Norman, H. Ding, M. Randeria, J.-C. Campuzano, T. Yokoya, T. Takeuchi, T. Takahashi, T. Mochiku, K. Kadowaki, P. Guptasarma, and D. G. Hinks, Nature (London) **392**, 157 (1998).
[17] P. Bourges (unpublished).
[18] A. A. Abrikosov, Phys. Rev. B **57**, 8656 (1998).
[19] A. A. Abrikosov, Phys. Rev. B **62**, 15 156 (2000).
[20] A. A. Abrikosov, Phys. Rev. B **52**, R15 738 (1995).
[21] A. A. Abrikosov, Phys. Rev. B **53**, R8910 (1996).
[22] Y. Sidis, C. Ulrich, P. Bourges, C. Bernhard, C. Niedermayer, L. P. Regnault, N. H. Andersen, and B. Keimer, Phys. Rev. Lett. **86**, 4100 (2001).
[23] J. E. Sonier, J. H. Brewer, R. F. Kiefl, R. I. Miller, G. D. Morris, C. E. Stronach, J. S. Gardner, S. R. Dunsiger, D. A. Bonn, W. N. Hardy, R. Liang, and R. H. Heffner, Science **292**, 1692 (2001).